A. NAGODE, G. KLANČNIK, M. BIZJAK, D. KOVAČEVIĆ, B. KOSEC,
E. DERVARIČ, B. ZORC, L. KOSEC

ISSN 0543-5846
METABK 52(1) 11-14 (2013)
UDC – UDK 669.14.018.298:669.18=111

STRUCTURAL AND THERMODYNAMIC ANALYSIS OF WHISKERS ON THE SURFACE OF GREY CAST IRON

Received – Prispjelo: 2012-04-18
Accepted – Prihvaćeno: 2012-08-15
Original scientific paper – originalni znanstveni rad

The paper focuses, first, on the characterization of the whiskers on the surface of grey cast iron and second, it gives an explanation of whiskers growth based on thermodynamic calculations. The whiskers were observed on the surface of hot plates for the electric stove after black-oxide-coating (blackening) performed the furnace at 650 °C in order to produce a protective layer mainly of magnetite (Fe_3O_4). However, the whiskers caused brown spots on dark grey surface and thus, the surface was aesthetically damaged. The investigations confirmed that whiskers are of hematite (Fe_2O_3); however, the thermodynamic calculations present that hematite may be formed as a result of the oxidation of magnetite if the partial pressure of oxygen is increased during the blackening.

Key words: whiskers, grey cast iron, magnetite (Fe_3O_4), hematite (Fe_2O_3)

INTRODUCTION

A surface of a hot plate made of grey cast iron used for the electric stove exhibits many brown stains (Figure 1) after black oxide coating (blackening). The blackening [1] is mainly used to produce a protective dark (grey) oxide layer [2,3] on the surface consisting predominantly of magnetite (Fe_3O_4); however, it also prevents against corrosion and abrasion, and since it has also decorative role the occurrence of brown stains on the surface is thus not acceptable [4]. Before blackening the grooves on the surface of the hot plate are made by turning [5-7] .

The black oxide coating process of hot plate was held in the furnace at 650 °C. For the appropriate atmosphere for producing a thin oxide layer on the surface of grey cast iron the wood was burned [8]. The maximum temperature in the furnace of 650 °C is reached after four hours, while the whole process lasts eight hours.

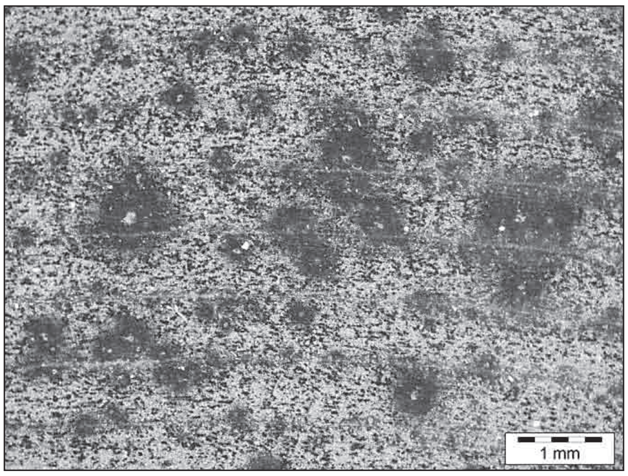

Figure 1 Brown stains on the surface of grey cast iron after blackening

EXPERIMENTAL

For the microstructural characterization of the brown stains on the surface of grey cast iron which have been observed after blackening a scanning electron microscope Jeol JSM 5610 equipped with energy dispersive x-ray spectrometer (EDXS) was used [9]. The accelerated voltage of electron beam was 20 keV. An x-ray diffraction analysis was also performed for phase identification. Thus, an x-ray diffractometer PANalytical X´Pert PRO (radiation wavelength CuKα_1 = 1,5406 Å) with Johansson monochromator for flat samples has been used.

RESULTS AND DISCUSSION

A detailed observation of the surface of grey cast iron after blackening using scanning electron microscope revealed that the surface with brown stains (Figure 1) is covered with whiskers [10-14] (Figure 2), while the surface where no brown stains have been observed shows typical oxide pattern (Figure 3) which reflects grain orientation of the base material.

Backscatter electron image (BEI) of the cross section of the sample covered with whiskers (Figure 4) shows, chemically, two different oxide layers on the base material (grey cast iron), i.e., the outer (light con-

A. Nagode, G. Klančnik, M. Bizjak, B. Kosec, E. Dervarič, B. Zorc, L. Kosec., Faculty of Natural Sciences and Engineering, University of Ljubljana, Slovenia D. Kovačević, Faculty of Technical Sciences, University of Novi Sad, Serbia

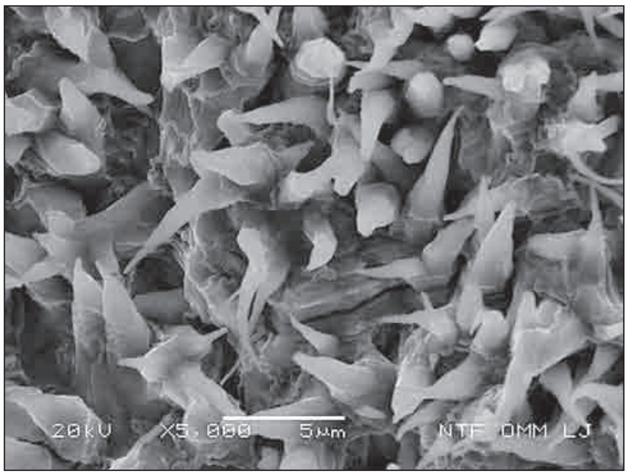

Figure 2 Surface of grey cast iron covered with whiskers; SEI

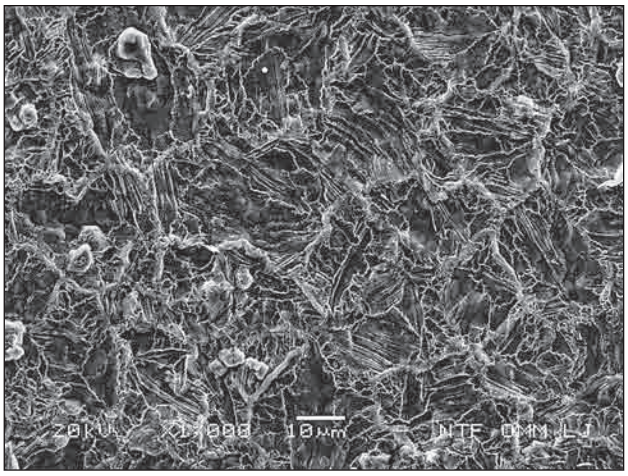

Figure 3 Typical oxide pattern after black oxide coating; SEI

trast) and the inner (dark contrast) oxide layers However, a detailed EDXS analysis (Table 1) shows that whiskers as well as the upper part of the outer oxide layer is composed of pure Fe-oxide, while in the lower oxide layer EDXS analysis indicates FeMn-oxides. The EDXS analysis of the inner oxide layer (dark contrast) confirms the presence of Fe, Mn and Cr; however, the increased content of Si indicates that the inner layer is composed of Si-rich Fe(MnCr) oxide.

In Figure 4 the internal oxidation of the matrix around the graphite flakes near the surface can also be seen. The internal oxidation actually consists of iron oxidation ($xFe + yO \rightarrow Fe_xO_y$) as well as graphite oxidation ($2C + O_2 \rightarrow 2CO$ or $C + O_2 \rightarrow CO_2$). The formation and growth of the Fe-oxide in the subsurface is promoted by oxygen penetration through the graphite boundaries with the metallic matrix [15, 16]. In order to show the element distribution on the cross section of the sample covered with whiskers an energy dispersive x-ray spectroscopy (EDXS) maps are presented. EDXS maps confirm above mentioned results of EDXS quantitative analysis. Distribution of carbon shows graphite flakes at the bottom of the image, however, at the top of the image the signal of C shows the signal C, Kα x-rays which come from the bakelite that the sample for metallographic preparation has been put in. The x-ray diffraction analysis was used for a phase identification of the surface covered with whiskers as well as for the surface without them. The analysis showed that the only difference between two XRD patterns lies in the ratio of the peak intensities between the hematite (Fe_2O_3) and the magnetite (Fe_3O_4). Namely, a detail from the XRD spectrum (2 theta = 32 ° - 2 theta = 36 °) of the surface covered with whiskers shows a higher peak-intensity ratio between the hematite (Fe_2O_3) and the magnetite (Fe_3O_4) (Figure 6a) in comparison to the x-ray diffraction pattern of the surface without whiskers (Figure 6b). Since the surface with brown stains is covered with whiskers this result indicates that the whiskers are composed of hematite (Fe_2O_3).

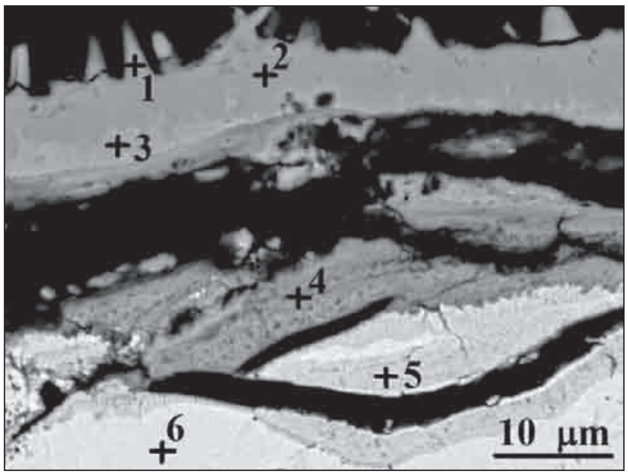

Figure 4 Cross section of the sample covered with whiskers; BEI

THERMODYNAMIC CALCULATIONS

For the calculation of particular phase diagram, Figure 7, the data for pure elements were taken from Dinsdale [17], for the substances data from Ansara [18]. Thermodynamic assessments on the Fe-O phase dia-

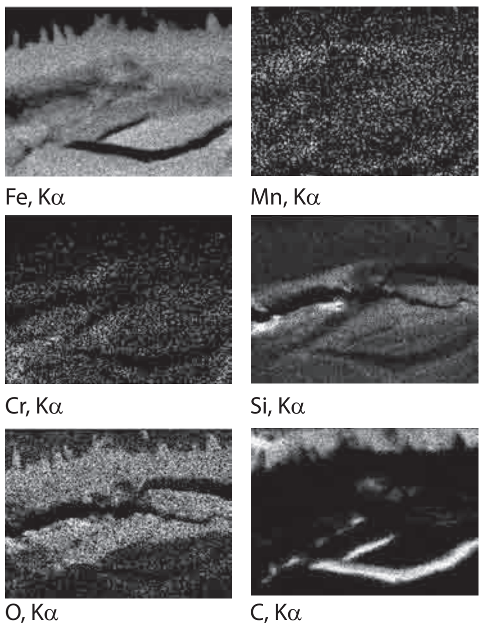

Figure 5 EDXS maps of Fe, Mn, Cr, Si O and C

Table 1 **EDXS analysis of the sample covered with whiskers in cross section /wt. %**

Site of interest	Fe	O	Mn	Si	Cr
1	93,5	6,5	-	-	-
2	95,9	4,1	-	-	-
3	96,0	1,9	1,1	-	-
4	95,9	3,1	0,4	0,3	0,3
5	95,8	0,6	0,7	2,2	0,6
6	97,4	-	0,6	1,3	0,7

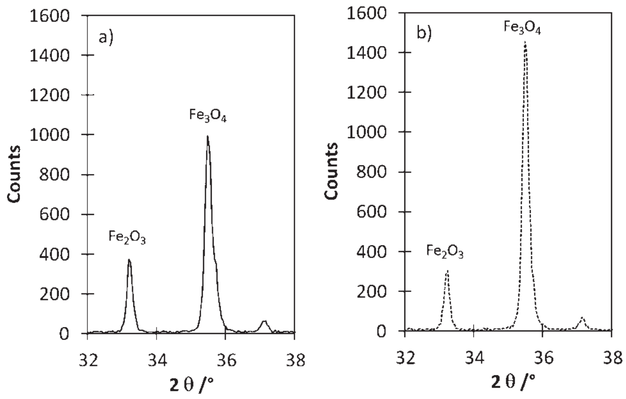

Figure 6 A detail of XRD spectrum of the surface; a) covered with whisker; b) without whiskers

gram were done by Sundman [19] and Selleby and Sundman [20]. The calculation of the phase diagram was done using Thermo-Calc software (TCW5).

The calculations were performed using equation 1 and equation 2. The activity of oxide was taken to be 1 as in the case of pure metal. The standard state of the gas is 1 atm. The equation for oxidation of pure metal is given with equation 1:

$$\frac{2u}{v} Me_{(s)} + O_2 = \frac{2}{v} Me_u O_{v(s)} \quad (1)$$

$$\Delta G = \Delta G^0 + RT \ln po_2^{-1}(eq.) = \Delta G^0 - RT \ln po_2(eq.) \quad (2)$$

$$2Fe(\mathrm{s}) + O_2 = 2FeO(\mathrm{s})$$
$$\Delta G^0 = -529\ 800 + 113{,}0T \quad (3)$$

$$1{,}5Fe(\mathrm{s}) + O_2 = 0{,}5Fe_3O_4(\mathrm{s})$$
$$\Delta G^0 = -553\ 400 + 148{,}0T \quad (4)$$

$$4Fe_3O_4(\mathrm{s}) + O_2 = 6Fe_2O_3(\mathrm{s})$$
$$\Delta G^0 = -498\ 900 + 281{,}3T \quad (5)$$

$$6FeO(\mathrm{s}) + O_2 = 2Fe_3O_4(\mathrm{s})$$
$$\Delta G^0 = -624\ 400 + 250{,}2T \quad (6)$$

where $\Delta G(J)$ and $\Delta G^0(J)$ represents the Gibbs energy change of the reaction when all reactants and products are at their respective arbitrarily states and the standard Gibbs energy of formation (equations 3-6). R is the gas constant (8,3144 $Jmol^{-1}K^{-1}$), T temperature (K) and po_2 (eq.) (atm) is equilibrium (dissociation) pressure of iron oxide. The calculations were done for equilibrium conditions, $\Delta G = 0$ Constant isobars at specific temperatures revealed large variations of dissociation pressures of iron oxides existing between different oxide regions. So, proper heating and cooling conditions (with controlled partial pressure-oxygen content inside the gas reservoir) are needed for controlled growth of oxides, Figure 7. If the value po_2 for a given atmosphere under consideration lies under the dissociation pressure of iron oxide po_2 (eq.), this oxide will dissociate into the oxygen and metal (or another oxide). On the contrary, if the value po_2 lies above the dissociation pressure of iron oxide po_2 (eq.), then the iron oxide is stable. So, increased partial pressure of oxygen relative to dissociation pressure at temperature of interest the formation of the hematite on the pre-existing magnetite is possible. The content of particular oxide (Fe_2O_3 on Fe_3O_4) is a time-dependant function.

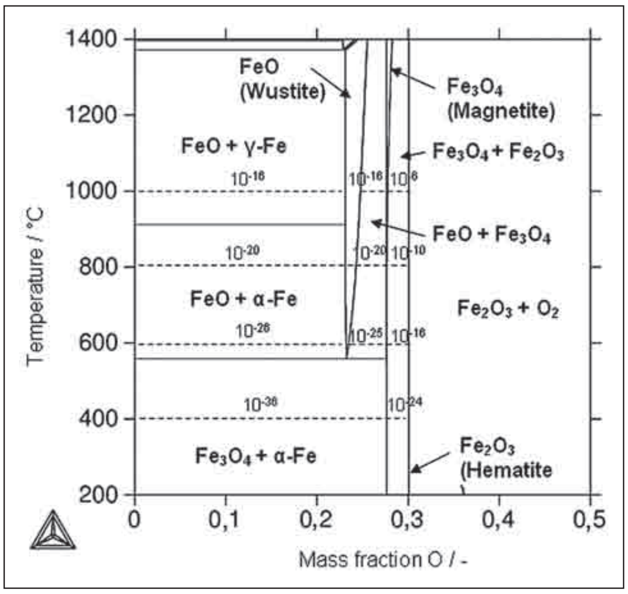

Figure 7 Fe-O phase diagram, and partial pressure of oxygen at 400 °C, 600 °C, 800 °C and 1000 °C

CONCLUSIONS

Whiskers growth on the surface of hot plates made of grey cast iron caused brown stains and thus, aesthetically damaged the surface. Scanning electron microscope (SEM) showed that whiskers were growing from the top oxide layer on the surface of grey cast iron. An EDXS analysis confirmed that the oxide on the surface of the grey cast iron consists, chemically, of three different types of oxides, i.e., whiskers and the outer oxide layer are pure Fe-oxide, below it is a narrow layer of FeMn-oxide, while the inner layer consists of Si-rich Fe(MnCr) oxide. An X-ray diffraction pattern of the surface covered with whiskers shows a higher Fe_2O_3/Fe_3O_4 peak-intensity ratio according to the x-ray diffraction pattern of the surface without them. This indicates that the whiskers are from hematite (Fe_2O_3).

REFERENCES

[1] N. Arab, M. Rahimi Nezhad Soltani, Journal of Applied Chemical Research, 9 (2009), 13-23.
[2] M. Gojić, J. Črnko, M. Kundak, L. Kosec, Kovové Materiály, 41 (2003), 158-166.
[3] M. Bizjak, A. Zalar, P. Panjan, B. Zorko, B. Praček, Applied Surface Science, 253 (2007), 3977-3981.
[4] A. Nagode, G. Klančnik, H. Schwarczova, B. Kosec, M. Gojić, L. Kosec, Engineering Failure Analysis, 23 (2012) 1, 82-89.
[5] J. Tušek, D. Klobčar, Journal of Mechanical Engineering, 50 (2004) 2, 94-103.
[6] I. Budak, M. Soković, M. Barišić, Measurement, 44 (2011) 6, 1188-1200.
[7] D. Klobčar, L. Kosec, B. Kosec, J. Tušek, Engineering Failure Analysis, 20 (2012) 1, 43 – 53.
[8] M. Medved, V. Malenković, E. Dervarič, Technics Technologies Education Management, 6 (2011) 2, 247-255.
[9] G. Kosec, A. Nagode, I. Budak, A. Antić, B. Kosec, Engineering Failure Analysis, 18 (2011) 1, 450-454.
[10] F. Tholence, M. Norell, Oxididation of Metals, 69 (2008), 13-36.
[11] B. Schmid, N. Aas, R. Ødegård, Oxidation of Metals, 57 (2002), 115-130.
[12] R. L. Higginson, G. Green, Corrosion Science, 53 (2011), 1690-1693.
[13] J. W. Kim, J.W. Choi, D.B. Lee, Metals and Materials International, 11 (2005), 131-134.
[14] A. Ivanič, S. Lubej, R. Rudolf, I. Anžel, Science and Engineering of Composite Materials, 18 (2011) 3, 181-186.
[15] J. Robertson, M.I. Manning, Materials Science and Technology, 5 (1989), 741-753.
[16] M. B. Lin, C. Jeng, A.A. Volinsky, Oxidation of Metals, 76 (2011), 161-168.
[17] A. T. Dinsdale, SGTE Data for Pure Elements, Calphad 15 (4) (1991), 317-425.
[18] I. Ansara, SGTE Substance Database (2000).
[19] B. Sundman, Journal of Phase Eguilibrium, 12 (1991), 127-140.
[20] M. Selleby, B. Sundman, Calphad 20 (1996), 381-392.

Note: The responsible translator for English language is Urška Letonja, MOAR, Podgora, Slovenia.